Journal of Sound and Vibration (2001) **243**(3), 475–501
doi:10.1006/jsvi.2000.3423, available online at http://www.idealibrary.com on IDEAL®

RESOLUTION OF THE TRANSIENT DYNAMIC PROBLEM WITH ARBITRARY LOADING USING THE ASYMPTOTIC METHOD

N. Berrahma-Chekroun and M. Fafard

GIREF and Department of Civil Engineering, Laval University, Quebec, Canada G1K 7P4

and

J. J. Gervais

GIREF and Department of Mathematics and Statistic, Laval University, Quebec, Canada G1K 7P4

(*Received* 1 *December* 1999, *and in final form* 11 *October* 2000)

Analysis of dynamic systems is more time consuming than of static ones due to the presence of inertia forces which vary in time. Equations of a dynamic system excited by arbitrary loads result in partial differential equations. The spatial part is discretized by the finite element method and the temporal part by implicit or explicit integration scheme. The time integration methods have already proved their effectiveness. However, in order to improve computing time for the resolution and quality of results, we present in this paper, a semi-analytical method based on an asymptotic method which allows to obtain a continuous solution for all time. In this method, the displacement field is expressed in power series. From this series, velocity and acceleration are easily computed. The load must be expressed also in series in the same manner as displacement. To do so, we use the Fourier integral to obtain an analytical function of an arbitrary load and then, we develop this function in power series using Taylor series. The dynamic asymptotic method (DAM) belongs to the conditionally stable-explicit methods. We apply this method in modal space in order to eliminate higher modes which influence the critical time (time segment length). Through numerical examples, we show better effectiveness of the asymptotic method compared to the Newmark method when we applied those schemes in the modal space.

1. INTRODUCTION

The asymptotic method (also called perturbation method) has been for a long time an efficient way to solve certain kinds of problems in various scientific fields. Its origin goes back to more than one century. This method was initially used in astronomy [1]. For example, this technique has been applied to discover the planet Neptune by the French astronomer Leverrier. In the beginning of the 1930s, Signori [2] has presented a technique of perturbation to transform a non-linear elastostatic problem in large displacement to a succession of linear problems. Koiter's Ph.D. thesis was on the stability of structure using perturbation method. This work has been resumed and supplemented by Budiansky [3] and Potier-Ferry [4].

The first application of the finite element method with a perturbation technique is due to Thompson and Walker [5]. They presented a general theory to solve a discrete non-linear problem by a perturbation method, and they applied it to the equilibrium problem of

0022-460X/01/230475 + 27 $35.00/0

a displacement-based finite element model. Several contributions were then proposed by Hangaï and Kawamata [2], and Connor and Morin [2], concerning in particular the applications. All this work was reviewed by Gallagher [6] and conclusions were not truly optimistic for the future of the asymptotic method in a finite element context.

The first interesting combination of the asymptotic method and the finite element method was proposed by Damil and Potier-Ferry [7] in a paper dealing with computation in perturbed bifurcation. Thereafter, Cochelin [2] showed that the asymptotic method could be used in a satisfactory way to solve problems of non-linear elasticity by using the finite element method.

Ammar [8] has extended the use of the asymptotic method to solve large rotations, non-linear problems where the displacement field is not expressed in polynomial form. Zahrouni [9] has presented numerical asymptotic algorithms to solve elastic shell problems in large rotations. He has also extended these algorithms to inelastic constitutive law.

Application of the asymptotic method to study the dynamic of structures is very recent. Fafard *et al.* [10] have developed a new method based on the asymptotic method to solve linear dynamic problems which they called dynamic asymptotic method (DAM). This method is based on the development of displacement, velocity and acceleration, in power series. The proposed method is conditionally stable because limited series are used. Fafard *et al.* [10] have shown that this method was more efficient than other conditionally stable explicit methods when it is applied in the modal space. The application of this method was limited to simple loading like constant load or linear load.

In this paper, we solve linear dynamic problems with arbitrary loading using the asymptotic method, by using the Fourier integral to obtain the loading as an analytical function. Using a finite element discretization scheme in space, the linear dynamic problem results in a set of ordinary differential equations of the form

$$[M]\{\ddot{u}(t)\} + [C]\{\dot{u}(t)\} + [K]\{u(t)\} = \{F(t)\}, \tag{1}$$

where $[M]$, $[C]$ and $[K]$ are, respectively, mass, damping and rigidity matrices of the structure, $\{u\}$ the nodal displacement vector and a dot denotes differentiation with respect to time t. At this stage, it is obvious that the use of a numerical technique to discretize the time domain is necessary. Equation (1) can be projected in the modal space using standard modal superposition techniques. If the full system is conserved, the time domain can be discretized using the standard Euler, second order explicit, or Newmark-β implicit schemes. In either case, the resulting discretized system can be written as

$$[\tilde{K}]\{u\} = \{R(t)\} \quad \{u(t + \Delta t)\} = \{u(t)\} + \{\Delta u\}, \tag{2}$$

where $[\tilde{K}]$ and $\{R(t)\}$ are, respectively, the effective matrix and the effective incremental load vector. Both definition of $[\tilde{K}]$ and $\{R(t)\}$ depend on the integration scheme. The vector $\{\Delta u\}$ is the incremental displacement vector to be added to the known solution at the time t, $\{u(t)\}$, to obtain $\{u(t + \Delta t)\}$. In all cases, the solution is obtained in an incremental manner which means that the nodal displacement, velocity and acceleration vectors are known only at certain points in the time domain (0, Δt, $2\Delta t, \ldots, n\Delta t$, etc.). Unfortunately, explicit methods are conditionally stable and very small time steps are often needed. Unconditionally stable implicit schemes permit the use of larger time steps; the size is governed only by accuracy considerations. Unfortunately, these schemes require a matrix factorization which means that larger computer core storage is needed and more operations per time step are required than with the central difference scheme. Also, to avoid the aliasing phenomenon, the time step must be less than or equal to the lowest period which participates in the response divided by 10 [11]. However, the asymptotic method gives

a continuous solution as function of time, its time step (time segment length) is computed automatically and it adapts according to the variation of the loading.

In the following sections, the solution of the transient dynamic problem with an arbitrary loading is presented. In order to get a polynomial form of loads, we develop the function obtained by Fourier integral, in Taylor series. Then, we will extend this technique to more complex problems, in order to be able to treat systems with several degrees of freedom by the asymptotic method.

2. PRESENTATION OF THE ASYMPTOTIC METHOD IN LINEAR DYNAMICS

2.1. BASIC CONCEPT OF THE ASYMPTOTIC METHOD

The resolution of a dynamic problem with the asymptotic method offers the advantage of expressing displacement and load in power series of time. The velocity and the acceleration are obtained by time differentiation of the displacement series. System (1) being linear with constant coefficients, the representation of the solution by a series is valid for any time t if the load is also representable by a power series. In other words, the expression of displacement in a series is written as

$$\{u(t)\} = \sum_{j=0}^{\infty} t^j \{u_j\}. \tag{3}$$

The vectors $\{u_j\}$ are the unknown vectors independent of time; vectors $\{u_0\}$ and $\{u_1\}$ represent the initial displacement and the initial velocity vectors respectively.

The first and second derivatives are easily computed using the series of $\{u(t)\}$

$$\{\dot{u}(t)\} = \sum_{j=1}^{\infty} j t^{j-1} \{u_j\}, \qquad \{\ddot{u}(t)\} = \sum_{j=2}^{\infty} j(j-1)\, t^{j-2} \{u_j\}. \tag{4}$$

By introducing these series into the equilibrium equations, we can find by recursiveness the unknown vectors $\{u_j\}$. Obviously, in order to group terms of the same power, the nodal loading vector must be converted into power series in the same manner as the displacement

$$\{F(t)\} = \sum_{j=0}^{\infty} t^j \{F_j\}, \tag{5}$$

where vectors $\{F_j\}$ contain the coefficients of the series (5).

By replacing the displacement, the velocity, the acceleration and the loading vectors according to their respective asymptotic expression, the dynamic equilibrium equations then becomes

$$[M] \sum_{j=2}^{\infty} j(j-1) t^{j-2} \{u_j\} + [C] \sum_{j=1}^{\infty} j t^{j-1} \{u_j\} + [K] \sum_{j=0}^{\infty} t^j \{u_j\} = \sum_{j=0}^{\infty} t^j \{F_j\}. \tag{6}$$

By grouping terms of the same power of t in equation (6), we obtain for $j = 2, \ldots, \infty$ the unknown vectors

$$\{u_j\} = \frac{1}{j(j-1)} [M]^{-1} (\{F_{j-2}\} - (j-1)[C]\{u_{j-1}\} - [K]\{u_{j-2}\}). \tag{7}$$

Since, in practice, we cannot compute all the terms of the series representing $u(t)$, we approach the solution by the series truncated at a certain order N:

$$\{u(t)\} = \sum_{j=0}^{N} t^j \{u_j\}. \tag{8}$$

By introducing this truncated series in the equilibrium equations (1), we obtain the residue

$$\{R(t)\} = t^{N-1}\{R_{N-1}\} + t^N\{R_N\} - \sum_{j=N+1}^{\infty} t^j\{F_j\}, \tag{9}$$

where

$$\{R_{N-1}\} = N[C]\{u_N\} + [K]\{u_{N-1}\} - \{F_{N-1}\} \neq 0,$$

$$\{R_N\} = [K]\{u_N\} - \{F_N\} \neq 0. \tag{10}$$

By considering that the loading is well represented by the truncated series $\sum_{j=0}^{N} t^j\{F_j\}$ the residue can be approximately estimated by

$$R(t) \approx t^{N-1}\{R_{N-1}\} + t^N\{R_N\}. \tag{11}$$

Since the vectors $\{R_{N-1}\}$and $\{R_N\}$ are generally different from zero, the residue will also be different from zero. Thus, this fact implies that the dynamic equilibrium of the structure will not be entirely satisfied. For N fixed, there exists a validity zone of the series beyond which the solution will not be valid. Consequently, to deduce the full solution for a given problem, the asymptotic method must be applied segment by segment. In each segment, we should calculate an error estimator of the solution to compute a critical time length to maintain a good precision of the approximation with the truncated series.

2.2. AUTOMATIC TIME SEGMENT COMPUTATION

Cochelin [2] has observed that asymptotic solutions incorporating two consecutive orders are very similar inside a validity zone; then they deviate one from the other at a certain time when they reach the limit of the validity zone. We can easily estimate this critical time in the following way:

$$\frac{\|\{u(t_{cr}^i + \tau)\}_{order\ N} - \{u(t_{cr}^i + \tau)\}_{order\ N-1}\|}{\|\{u(t_{cr}^i + \tau)\}_{order\ N} - \{u(t_{cr}^i)\}\|} \leqslant \varepsilon, \quad t_{cr}^i \leqslant \tau \leqslant t_{cr}^{i+1}, \tag{12}$$

where neglecting higher order terms in the denominator of equation (12), we obtain

$$t_{cr}^{i+1} = t_{cr}^i + \left(\varepsilon \frac{\|\{u_1\}\|}{\|\{u_N\}\|}\right)^{1/(N-1)} \quad \text{if } \|\{u_1\}\| \neq 0. \tag{13}$$

The vector $\{u_1\}$ corresponds to the velocities at the end of the previous segment, it is related therefore to the initial conditions of the current time segment. In the case where $\{u_1\}$ is zero, the critical time segment can be obtained by

$$t_{cr}^{i+1} = t_{cr}^i + \left(\varepsilon \frac{\|\{u_2\}\|}{\|\{u_N\}\|}\right)^{1/(N-2)}. \tag{14}$$

2.3. STABILITY STUDY

It is well known that explicit time integration schemes are conditionally stable [12]. The DAM is an explicit method and thus, is conditionally stable. Stability analysis of this method has been presented in references [10, 13].

3. TAYLOR DEVELOPMENT OF THE LOADING VECTOR

To solve linear dynamics problems by the asymptotic method, we must express the loading in power series in the same manner as the displacement field. For that purpose, we will develop the loading vector in a Taylor series in order to obtain a polynomial representation of the load. However, in dynamic analysis and particularly in seismic analysis, the loading function is rarely given by an explicit analytical function, which prevents us to compute its Taylor series explicitly. The most used technique to represent an arbitrary loading is the transformation using Fourier series. This technique can be easily applied to periodic loading. If the load is not periodic, we can add at the end of this loading a zero load, long enough to prevent the recurrence of the load. This technique has been tested and we find that it is less advantageous when compared to the next technique presented in this paper.

To represent arbitrary non-periodic loads, we use the Fourier integral. Thereafter, we will extend this technique for more complex problems, in order to be able to treat systems with several degrees of freedom subjected to an arbitrary loading by the asymptotic method.

3.1. REPRESENTATION OF THE MODAL LOADING BY FOURIER SERIES

A function $f(t)$ defined in the interval $(-L, L)$ and given outside this interval by $f(t + 2L) = f(t)$, has a period of $2L$ (Figure 1). The Fourier series of a $2L$- periodic function $f(t)$ is defined as

$$f(t) = a_0 + \sum_{n=1}^{\infty} (a_n \cos \Omega_n t + b_n \sin \Omega_n t) \quad \text{with} \quad \Omega_n = n\pi/L, \tag{15}$$

where the Fourier coefficients a_0, a_n and b_n are $(n = 1, 2, \ldots)$

$$a_0 = \frac{1}{L}\int_{-L}^{L} f(t)\,\mathrm{d}t, \qquad a_n = \frac{2}{L}\int_{-L}^{L} f(t)\cos \Omega_n t\,\mathrm{d}t, \qquad b_n = \frac{2}{L}\int_{-L}^{L} f(t)\sin \Omega_n t\,\mathrm{d}t. \tag{16}$$

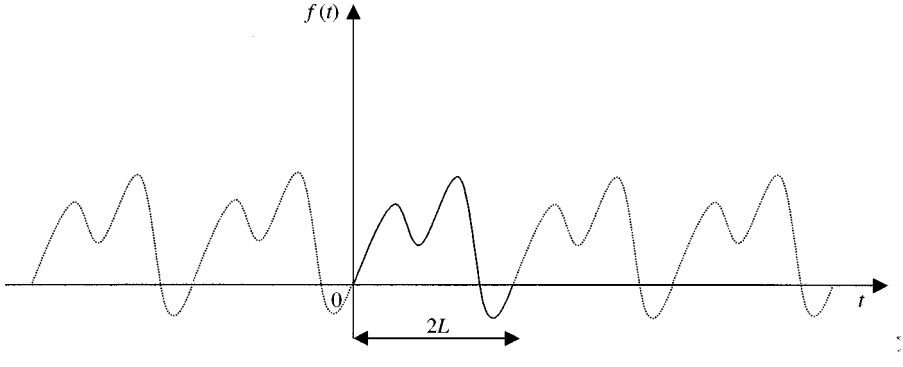

Figure 1. Periodic function.

Since the Taylor series of the harmonic functions like the cosinus and the sinus functions are known, we are able to develop a Taylor series for any combination of harmonic functions. The Taylor series of the cosinus and sinus functions in the neighborhood of the critical point t_{cr} are

$$\cos(\Omega_n(t_{cr}+\tau)) = \cos(\Omega_n t_{cr}) - \sin(\Omega_n t_{cr})\frac{\Omega_n\tau}{1!} - \cos(\Omega_n t_{cr})\frac{(\Omega_n\tau)^2}{2!} + \sin(\Omega_n t_{cr})\frac{(\Omega_n\tau)^3}{3!} + \cdots \tag{17}$$

and

$$\sin(\Omega_n(t_{cr}+\tau)) = \sin(\Omega_n t_{cr}) + \cos(\Omega_n t_{cr})\frac{\Omega_n\tau}{1!} - \sin(\Omega_n t_{cr})\frac{(\Omega_n\tau)^2}{2!} - \cos(\Omega_n t_{cr})\frac{(\Omega_n\tau)^3}{3!} + \cdots. \tag{18}$$

Replacing these two expressions in the Fourier series (15), we find

$$f(t_{cr}+\tau) = f_0 + f_1\tau + f_2\tau^2 + f_3\tau^3 + \cdots \tag{19}$$

with

$$f_0 = a_0 + \sum_{n=1}^{\infty}[a_n\cos(\Omega_n t_{cr}) + b_n\sin(\Omega_n t_{cr})],$$

$$f_i = \left(\sum_{n=1}^{\infty}[a_n\cos(\Omega_n t_{cr}) + b_n\sin(\Omega_n t_{cr})]\right)\frac{(-1)^{i/2}(\Omega_n)^i}{i!}, \quad i = even,$$

$$f_i = \left((-1)^{(i+1)/2}\sum_{n=1}^{\infty}a_n\sin(\Omega_n t_{cr}) + (-1)^{(i-1)/2}\sum_{n=1}^{\infty}b_n\cos(\Omega_n t_{cr})\right)\frac{(\Omega_n)^i}{i!}, \quad i = odd. \tag{20}$$

Having the Taylor coefficients of the loading $f(t)$, we can then compute the coefficients of the displacement defined by equation (7).

3.2. RESOLUTION OF A SINGLE-DEGREE-OF-FREEDOM SYSTEM (s.d.o.f)

To illustrate the application of Fourier series to an undamped forced vibration problem, we will study a single-degree-of-freedom system. We use an asymptotic development with 30 terms. The tolerance to compute the critical time is equal to 10^{-4}. The data of this problem are $k = 4$, $m = 1$ and the initial conditions are set to ($u_0 = u_1 = 0$). The load is a triangular function; we use 15 terms of the Fourier series ($n = 15$) to approximate the loading. The differential equation of the system is the following one:

$$\ddot{u} + 4u = \begin{cases} t, & t \leqslant 4, \\ -t + 8, & 4 \leqslant t \leqslant 8 \end{cases} \tag{21}$$

and its analytical solution can be easily obtained:

$$u(t) = \begin{cases} 0{\cdot}25t - 0{\cdot}125\sin(2t), & t \leqslant 4, \\ -0{\cdot}123\cos(2t-8) + 0{\cdot}268\sin(2t-8) - \frac{1}{4}t + 2, & 4 \leqslant t \leqslant 8. \end{cases} \tag{22}$$

Figure 2 shows that the results obtained with the asymptotic method associated with Fourier series are practically exact. We can thus say that this approach gives good results. Furthermore, this approach can be applied to problems of several degrees of freedom with an arbitrary periodic loading, since the solution of a problem expressed in the modal space is similar to equation (21). Nevertheless, this technique presents some disadvantages that we will depict in section 3.4.

3.3. REPRESENTATION OF THE MODAL LOADING BY THE FOURIER INTEGRAL

3.3.1. *General case*

We want to extend the representation of a non-periodic loading using a similar technique as in section 3.2. Let us consider the example of an arbitrary non-periodic loading as shown in Figure 3.

If we want to represent this function by Fourier series, it is necessary to take the period $(2L)$ large enough to represent this function as shown in Figure 4. It is obvious that the repetitive parts can perturb the solution if the total time of the analysis is larger than the period. To completely eliminate the repetitiveness of the basic loading, we must let the period $(2L)$ go up to infinity.

Let $f(t)$ be a function with a period $(2L)$ that we can represent by Fourier series as

$$f(t) = a_0 + \sum_{n=1}^{\infty} (a_n \cos \Omega_n t + b_n \sin \Omega_n t). \tag{23}$$

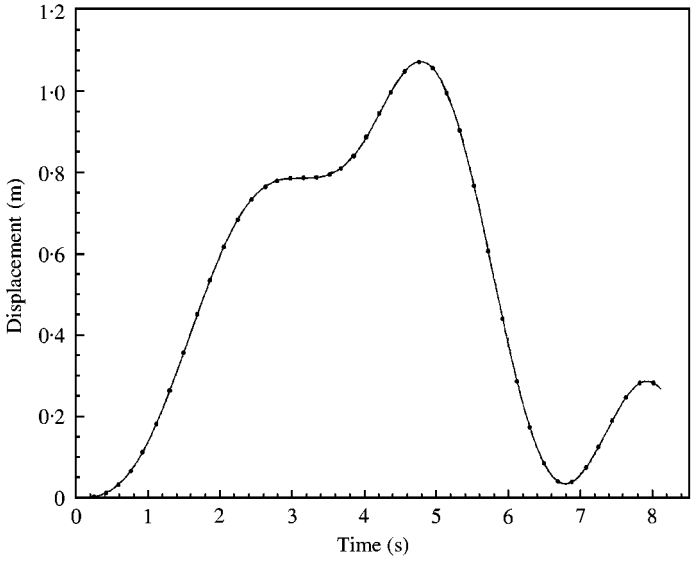

Figure 2. The single-degree-of-freedom system response using Fourier series: —•—, DAM solution; ——, analytical solution.

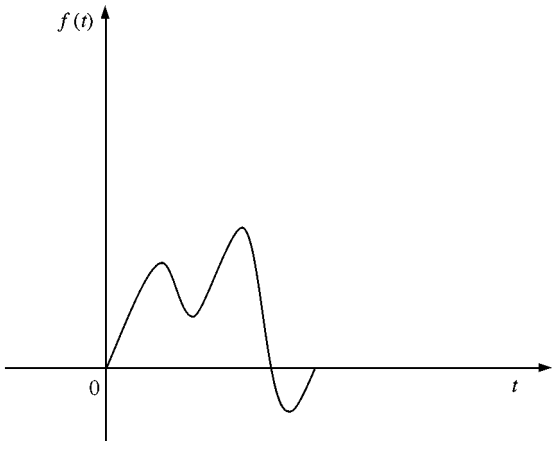

Figure 3. Non-periodic function.

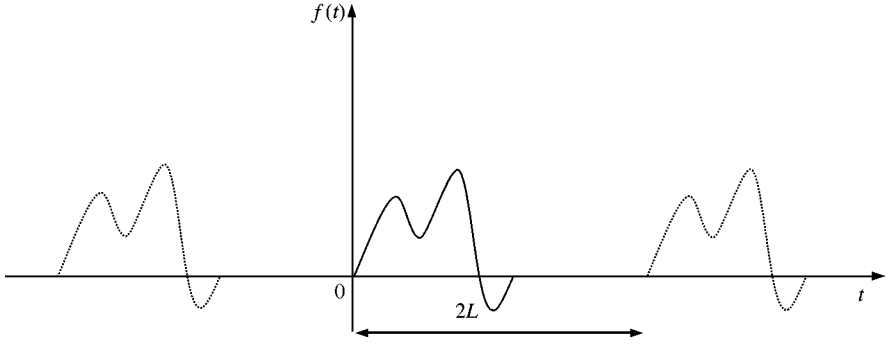

Figure 4. A representation of a non-periodic function like a periodic function.

In order to see what happens when this period approaches infinity, we replace the expressions of a_0, a_n and b_n in the above equation and the sum by an integral as follows:

$$f(t) = \int_0^\infty [A(\Omega) \cos \Omega t + B(\Omega) \sin \Omega t] \, \mathrm{d}\Omega \tag{24}$$

with

$$A(\Omega) = \frac{1}{\pi} \int_{-\infty}^{\infty} f(v) \cos \Omega v \, \mathrm{d}v, \quad B(\Omega) = \frac{1}{\pi} \int_{-\infty}^{\infty} f(v) \sin \Omega v \, \mathrm{d}v. \tag{25}$$

This is the representation of $f(t)$ by a so-called Fourier integral.

3.3.2. *Representation of a linear loading by the Fourier integral*

An arbitrary load can be represented by a piecewise linear function; it is a juxtaposition of linear segments like the one appearing in Figure 5. We can estimate the expression of the Fourier integral for this interval of time $[\alpha, \beta]$ and sum all terms of the function.

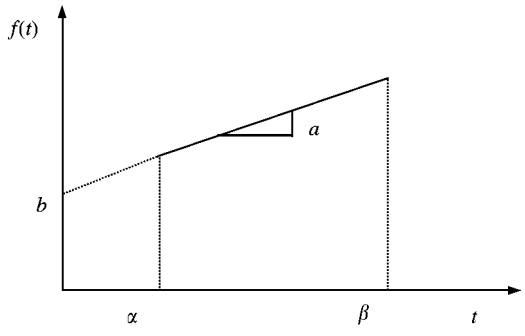

Figure 5. Linear load.

By calculating the two integrals (25) for $f(t) = at + b$ and replacing them in equation (24), the expression of the Fourier integral of $f(t)$ becomes

$$f(t) = \frac{1}{\pi\ell}\,[\,-a\cos(\ell(t-\beta)) + a\cos(\ell(t-\alpha)) - a\ell t\,Si(\ell(t-\beta))$$

$$+ a\ell t\,Si(\ell(t-\alpha)) - a\ell b\,Si(\ell(t-\beta)) + a\ell b\,Si(\ell(t-\alpha))], \tag{26}$$

where $Si(t) = \int_0^t (\sin(x)/x)\,\mathrm{d}x$ and ℓ is the upper limit of the Fourier integral. As the function $Si(t)$ cannot be computed explicitly, we used the Chebyshev series [14].

Having obtained the loading expression for a line segment using equation (26), we must express it in a Taylor series:

$$f(t_{cr} + \tau) = \sum_{j=0}^{\infty} \frac{\tau^j}{j!} f^{(j)}(t_{cr}), \tag{27}$$

where upper script (j) means jth derivative.

3.3.3. *Representation of discrete loading by Fourier integral*

For a discrete arbitrary loading (Figure 6) made of a set of line segments, equation (26) is written in the following way:

$$f(t) = \sum_{i=1}^{Np-1} [\,-a_i\cos(\ell(t-\alpha_{i+1})) + a_i\cos(\ell(t-\alpha_i)) - a_i\ell t\,Si(\ell(t-\alpha_{i+1}))$$

$$+ a_i\ell t\,Si(\ell(t-\alpha_i)) - a_i\ell b_i Si(\ell(t-\alpha_{i+1})) + a_i\ell b_i Si(\ell(t-\alpha_i))]/(\pi\ell), \tag{28}$$

where N_p represents the number of points of the loading curve.

3.3.4. *Resolution of a single-degree-of-freedom system*

In this example, we will find the solution to the problem considered in section 3.2 using the Fourier integral with an upper limit (ℓ) equal to 5 rad/s. We use the same parameters for the asymptotic method as those used in section 3.2. Thus, we can compare the results obtained using the Fourier series to those obtained by using the Fourier integral.

Figure 7 represents the analytical solution and the one obtained by the asymptotic method using the Fourier integral. We can clearly observe that the two curves are in good

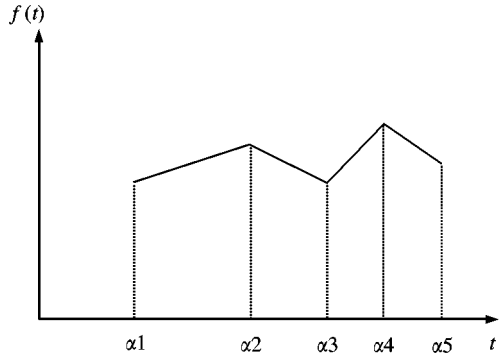

Figure 6. Discrete loading.

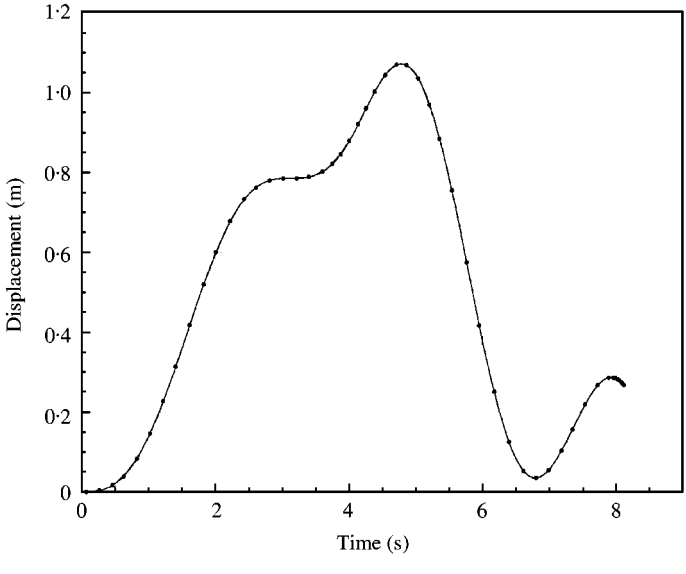

Figure 7. The single-degree-of-freedom system response using the Fourier integral: —•—, DAM solution; ——, analytical solution.

agreement. Then, we conclude that the technique of the Fourier integral can be used with the asymptotic method for a single-degree-of-freedom system.

3.4. COMPARISON BETWEEN THE FOURIER INTEGRAL AND FOURIER SERIES

As we mentioned in section 3.1, Fourier series are used to represent periodic functions. When the load is non-periodic, we must take a larger period than the time of analysis of the problem to avoid the return of the load. However, with the Fourier integral, we can express any function that it is periodic or not, which represents an advantage.

Besides, the load is generally represented in discrete forms. Using Fourier series to represent this type of loading, constrains us to compute series with several harmonics for each line segment representing the load. This approach is time consuming. On the other

TABLE 1

Computing time and critical times

	Fourier integral $\ell = 15$ rad/s	Fourier series $n = 15$	Ratio (1/2)
Relative (CPU) time	0·37	1	
Critical time (s)	2·52	1·90	1·33
	2·40	1·97	1·22
	1·95	1·93	1·01
	2·33	2·05	1·14
Mean critical time (s)	2·30	1·96	1·17

hand, with the Fourier integral, we just have to compute expression (24) for each segment. To illustrate the advantages of the Fourier integral used with the asymptotic method when compared to the use of Fourier series, we present in Table 1 some results obtained from the example presented in sections 3.2 and 3.3.4. We can observe that segments length are larger using the Fourier integral and the latter is less time consuming than the asymptotic method using Fourier series.

4. APPLICATIONS WITH SEVERAL DEGREES OF FREEDOM

4.1. VALIDATION AND PERFORMANCES OF THE ASYMPTOTIC METHOD

In this example, we study the frame in Figure 8 subjected to the Pacoima earthquake (Figure 9) in the horizontal direction. The objective is to demonstrate that the asymptotic method converges towards the exact solution and that it requires fewer steps than the Newmark-β integration method to obtain all the solution branches. Thus, the response of the structure is calculated by both methods: the Newmark-β method (with $\beta = 1/4$ and $1/6$) and the asymptotic method. We present thereafter the lateral displacement of the node (7) located at the top of the frame in order to compare those methods. The structural damping is neglected. The frequency of the upper limit of the Fourier integral is 120 rad/s. We use an asymptotic development with 29 terms. Each beam and column is meshed with a single element. The geometry and the physical characteristics of the structure are given in Figure 8.

We have computed the first six relative modal masses of the structure in order to choose the number of modes that must be included in the response. The first three relative modal masses are 86·79, 10·71 and 2·49%, which account for practically 100%. These first three modes have significant modal masses and thus contribute significantly to the response of the structure in the modal space [11]. Thus, we will use these first three modes for computing displacements of the structure. For the choice of the time step for the Newmark-β method, it is recommended to take one equal to the tenth of the smallest period included in the subspace of the structure [12]; thus, we find $\Delta t = 0{\cdot}0065$ s. The Pacoima earthquake was recorded with a time step of 0·02 s. To avoid the aliasing phenomenon (due to the fact that $0{\cdot}02/0{\cdot}0065 = 3{\cdot}07$), we have taken a time step equal to $0{\cdot}02/4 = 0{\cdot}005$ s (equivalent to $T_3/13$). For the explicit scheme, the stability criterion [12] is $\Delta t \leqslant 0{\cdot}55T_3 = 0{\cdot}036$ s, and consequently by taking $\Delta t = 0{\cdot}005$ s, we will remain inside the stability zone. The tolerance chosen to compute the critical time of the asymptotic method is 10^{-9}. Displacement versus time of the node (7) is plotted in Figures 10(a–f).

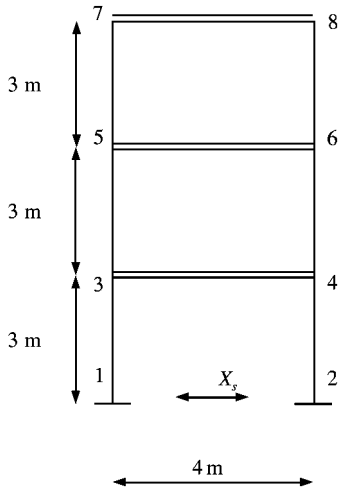

Figure 8. Frame subjected to Pacoima earthquake: $\rho = 7870\,\text{kg/m}^3$, $E = 2{\cdot}0 \times 10^{11}\,\text{N/m}^2$, $I_{Beam} = 100{\cdot}0 \times 10^{-6}\,\text{m}^4$, $I_{Column} = 51{\cdot}6 \times 10^{-6}\,\text{m}^4$, $A_{Beam} = 8{\cdot}0 \times 10^{-2}\,\text{m}^2$, $A_{Column} = 6{\cdot}92 \times 10^{-2}\,\text{m}^2$.

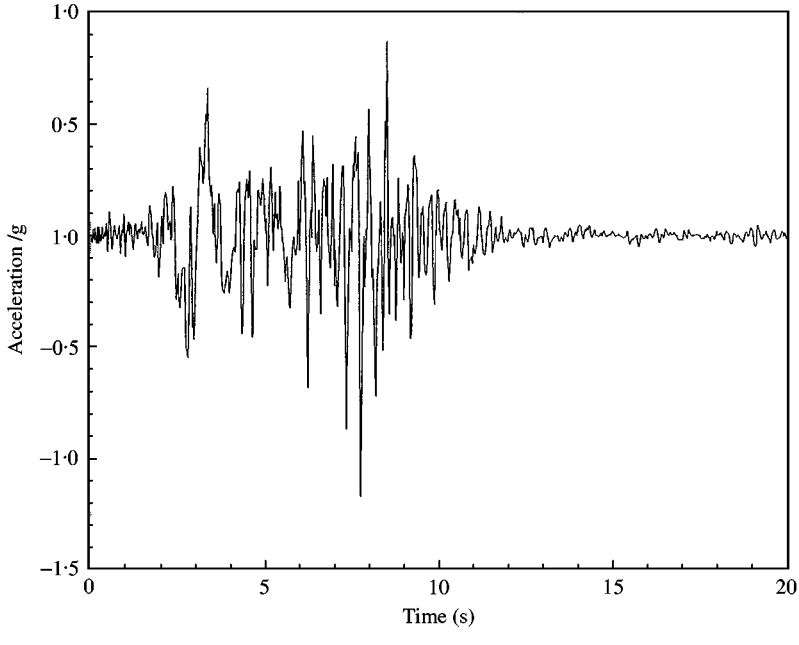

Figure 9. Pacoima earthquake recording.

By examining Figure 10(a) and 10(b), we note that the solutions obtained by the asymptotic method and the Newmark-β method with explicit and implicit schemes are identical during the first 10 s of the analysis. We also note that the solution calculated by

Figure 10. Horizontal displacement of the node (7) computed using DAM and the Newmark method ($\Delta t = 0{\cdot}005$ s): —○—, Newmark ($\beta = 1/6$); —◇—, Newmark ($\beta = 1/4$); ——, DAM. (a) $0 < \text{time} < 4$; (b) $4 < \text{time} < 10$; (c) $10 < \text{time} < 14$; (d) $14 < \text{time} < 17$; (e) $17 < \text{time} < 19$; (f) $19 < \text{time} < 20$.

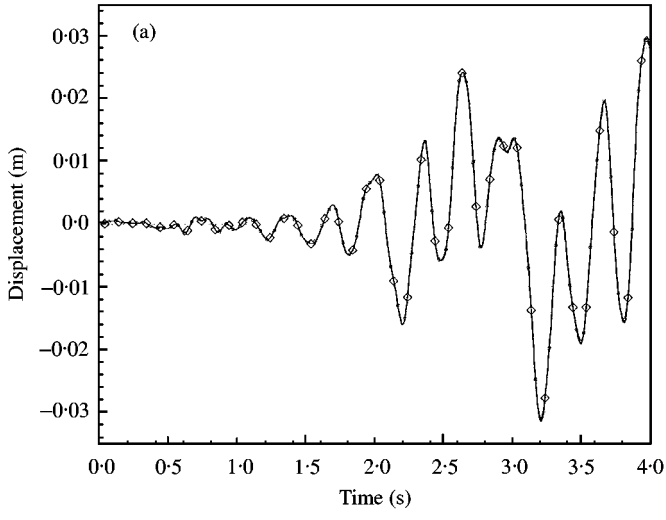
(a)
0·03
0·02
0·01
0·0
−0·01
−0·02
−0·03
Displacement (m)
0·0 0·5 1·0 1·5 2·0 2·5 3·0 3·5 4·0
Time (s)

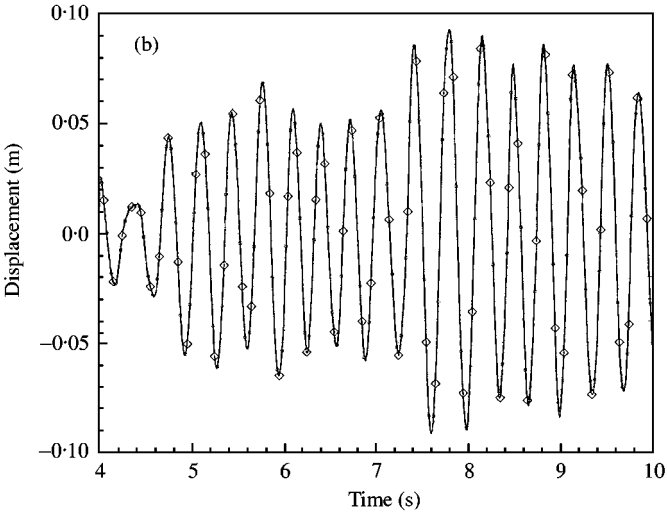
(b)
0·10
0·05
0·0
−0·05
−0·10
Displacement (m)
4 5 6 7 8 9 10
Time (s)

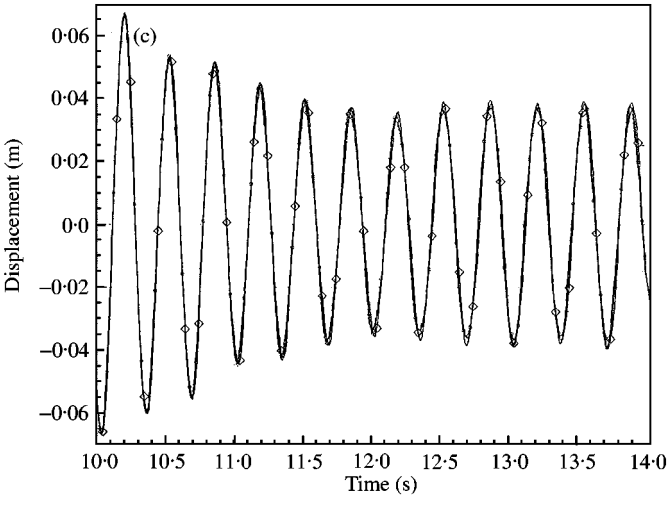
(c)
0·06
0·04
0·02
0·0
−0·02
−0·04
−0·06
Displacement (m)
10·0 10·5 11·0 11·5 12·0 12·5 13·0 13·5 14·0
Time (s)

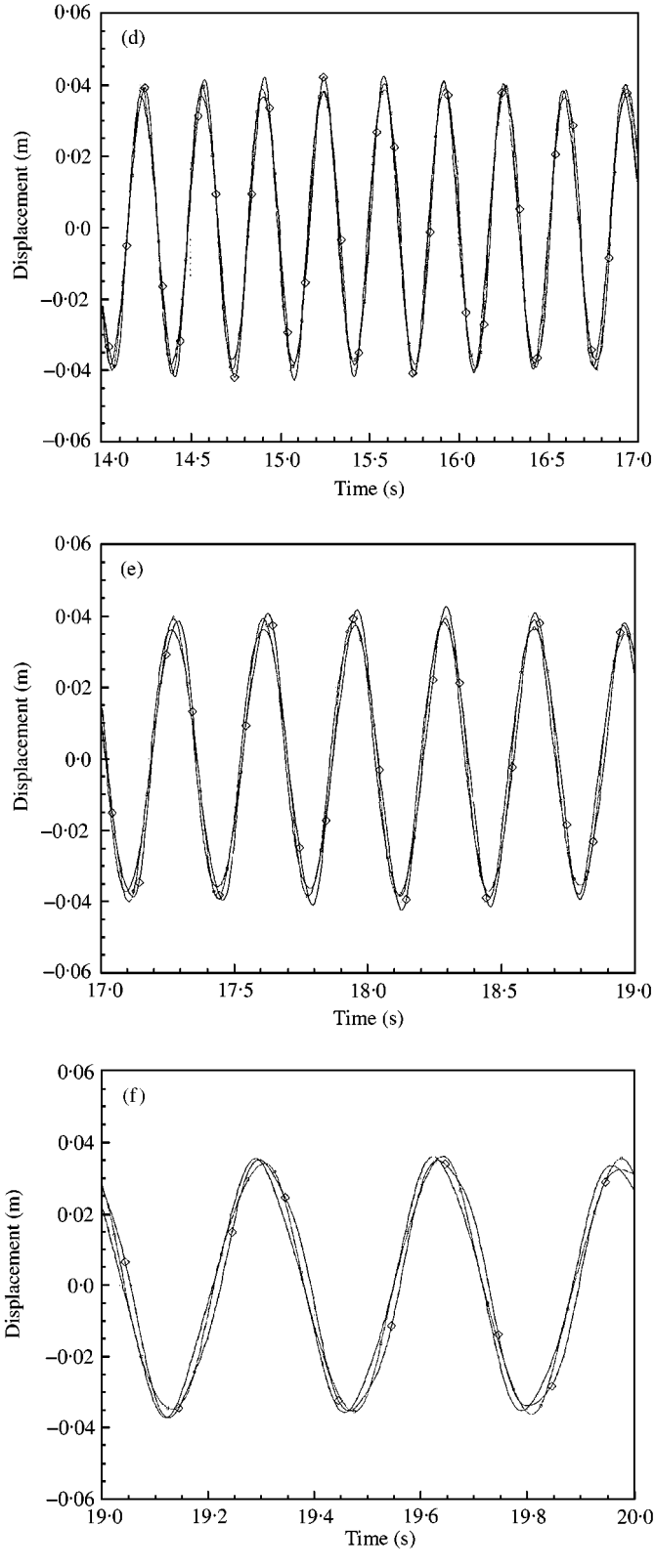

Figure 10. Continued.

using the implicit scheme starts to shift slightly from the two other solutions beyond the tenth second. The solution obtained with the conditionally stable scheme starts to shift from the one obtained using the asymptotic method from the 14th second. At the end of the analysis, we clearly see from Figure 10(f) that the three solutions are not identical.

In order to check which of the three numerical solutions gives the better approximation of the exact solution, we decrease the time step of the Newmark-β method for the two integration schemes to obtain more precise solutions. We note that as we decrease the time steps, the Newmark-β solutions approach the asymptotic method solution; we thus deduce that the developed method gave an excellent approximation of the exact solution. We note that the results obtained by the Newmark-β method with a time step of 0·02 s are very acceptable from an engineering point of view.

4.2. DYNAMIC STUDY OF A BRIDGE BOX

In this section, we study a concrete bridge subjected to the El-Centro earthquake (May 18, 1940) in its vertical direction (Figure 11). The objective of the analysis is to evaluate the performance of the asymptotic method compared to the Newmark-β method.

This bridge box has three consecutive continuous spans [15]. Figure 12 shows dimensions of the three spans. We illustrate in Figure 13 a transversal section of the bridge and in Figure 14 a plan view. The bridge is meshed with beam finite elements and shell finite elements. The bridge mesh is shown in Figure 15. It contains 1736 elements, 1622 nodes and 9732 degrees of freedom.

The number of modes which must be included in the response has been selected by computing the relative modal masses of each bridge modes (Figure 16). They are presented in Table 2. We note from this table that it is the third frequency which has the greatest modal mass and, thus, it will contribute significantly to the response. Consequently, we will

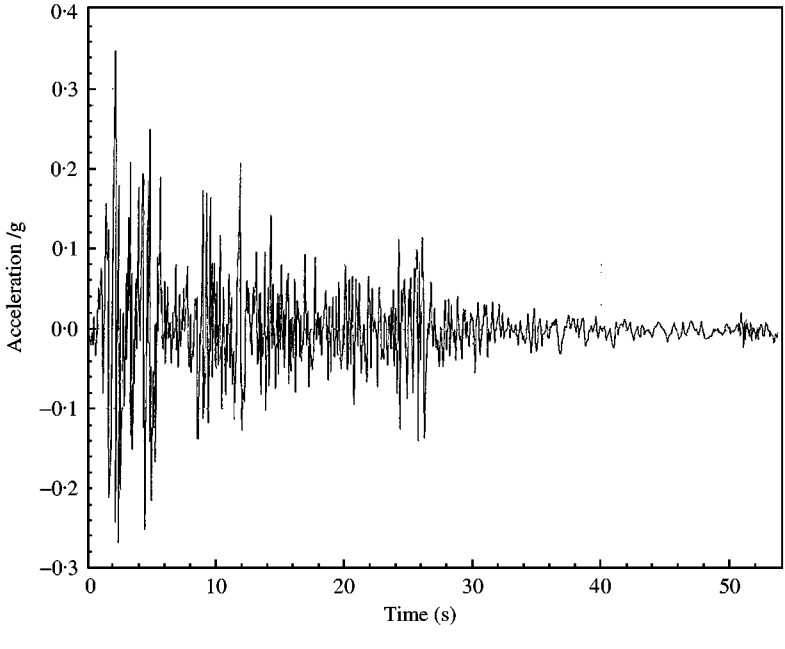

Figure 11. El-Centro earthquake recording.

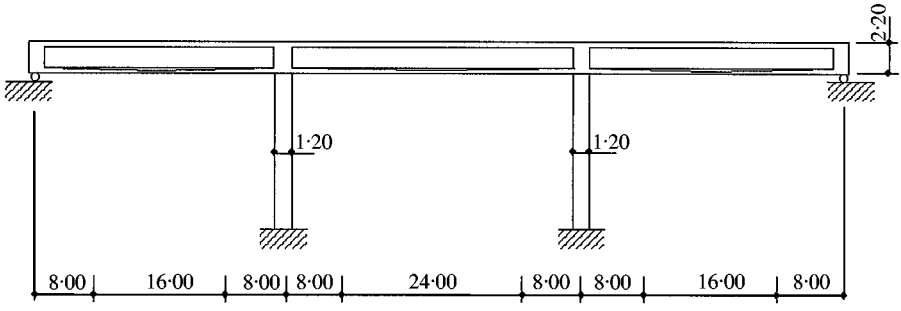

Figure 12. Longitudinal section.

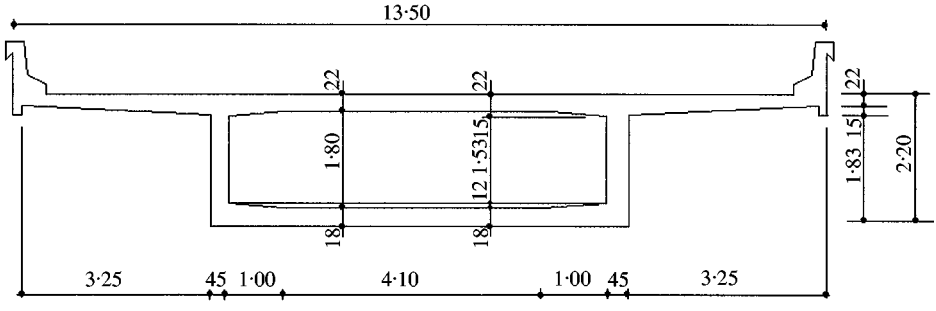

Figure 13. Transversal section.

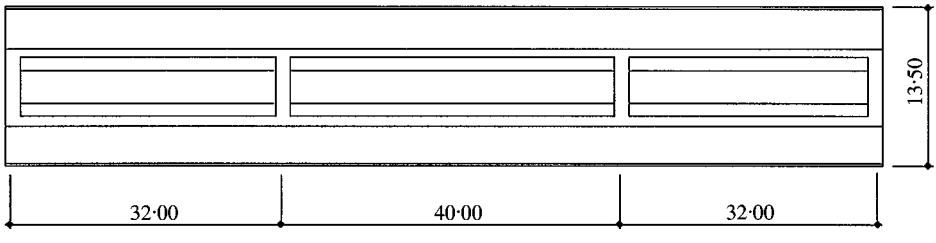

Figure 14. Plan view.

take the first three modes for the computation of the response. We estimate that the modal analysis gives satisfactory results when the modal masses selected account for at least 90% of the structure total mass. In our case, we do not take account of this fact since we are interested more in the numerical aspect of the method than the physical one.

4.3. CHOICE OF THE UPPER LIMIT OF THE FOURIER INTEGRAL

We know that if we underestimate the value of the upper limit in the Fourier integral, we will generate less accurate results. To determine an acceptable value of this upper limit and to see the effect of this frequency on the response, we have varied this frequency as follows: 30, 40, 60, 90 and 120 rad/s. We have taken 29 terms for the displacement series and a tolerance of 10^{-8} for the computing of critical time. The displacement at the center of the bridge is obtained for the selected upper limit of the Fourier integral (Figure 17).

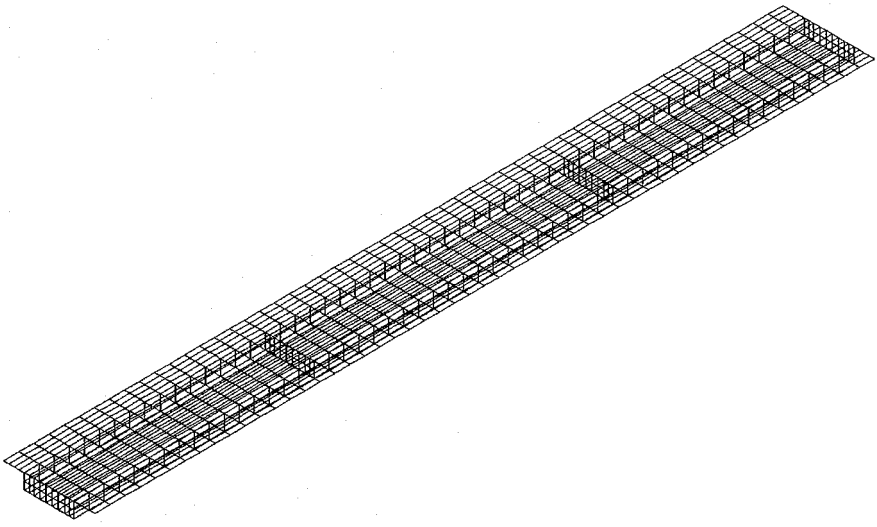

Figure 15. Bridge grid.

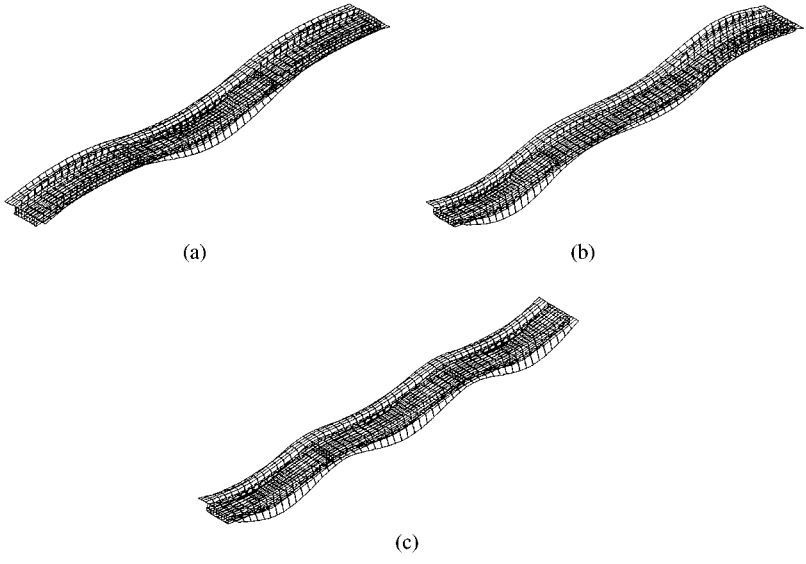

Figure 16. The first three modes included in the response: (a) first mode, (b) second mode, (c) third mode.

We observe that the curves obtained with frequencies of 60, 90, 120 rad/s are very close to each other; on the other hand, the ones obtained with 30 and 40 rad/s are far from the other curves. Hence, for the following, we take the value of 120 rad/s for the Fourier integral upper limit.

We will compute displacements of the bridge by the Newmark-β method with an explicit scheme and the asymptotic method projected in modal space. We will use an asymptotic development of 29, 20, 15 and 10 terms in order to see their influence on the computing time. The choice of the time step for the Newmark-β method with linear acceleration will primarily depend on the smallest period who participates in the response. In this case,

TABLE 2

Frequencies and modal masses

	Frequency (Hz)	Period (s)	Relative modal mass (%)
Mode 1	3·39	0·295	0·240
Mode 2	4·98	0·201	0·004
Mode 3	5·90	0·17	57·192
Mode 4	7·81	0·128	0·010
Mode 5	8·96	0·112	0·039
Mode 6	9·12	0·110	0·047
Mode 7	9·99	0·1	0·000
Mode 8	11·4	0·0877	0·000
Mode 9	12·6	0·0795	0·011
Mode 10	12·9	0·0776	0·092
			Total = 57·635

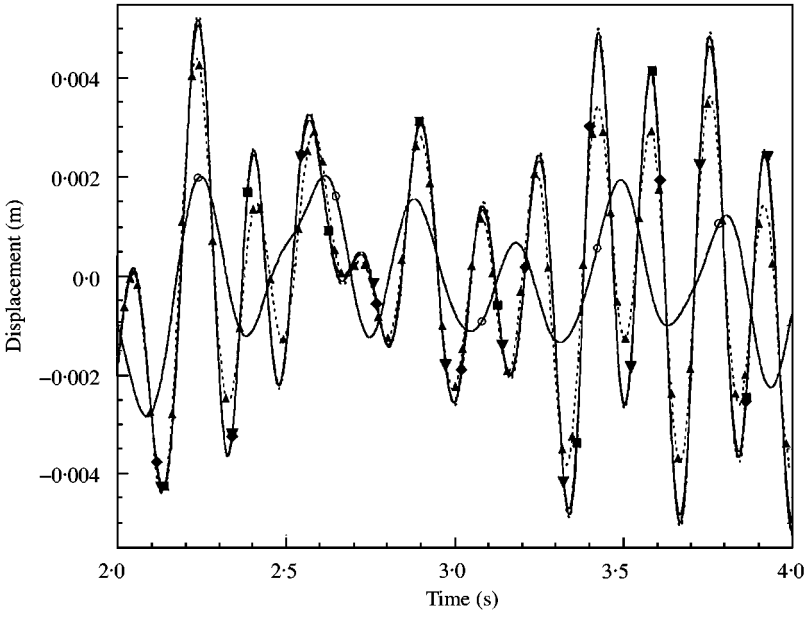

Figure 17. Choice of the upper limit of the integral: —○—, $\ell = 30$ rad/s; ----▲----, $\ell = 40$ rad/s; —◆—, $\ell = 60$ rad/s; ----▼----, $\ell = 90$ rad/s; —■—, $\ell = 120$ rad/s.

although a time step lower than $0{\cdot}55T_3$ is sufficient to guarantee the stability of the method, overall, a time step corresponding to $T_3/10$ is appropriate. The El-Centro recording was made for a time step of 0·02 s. To avoid the aliasing phenomenon (because 0·02/0·017 = 1·17), we have thus taken a time step equal to 0·02/2 = 0·01 (equivalent to $T_3/17$).

We first compute the bridge displacements using a Rayleigh damping equal to 5% for the first three modes of the structure. Figures 18(a–e) give the vertical displacement at the center of the bridge versus time for the two methods.

We note from those figures that the solution obtained by the asymptotic method and the Newmark-β method are in good agreement within the interval of analysis.

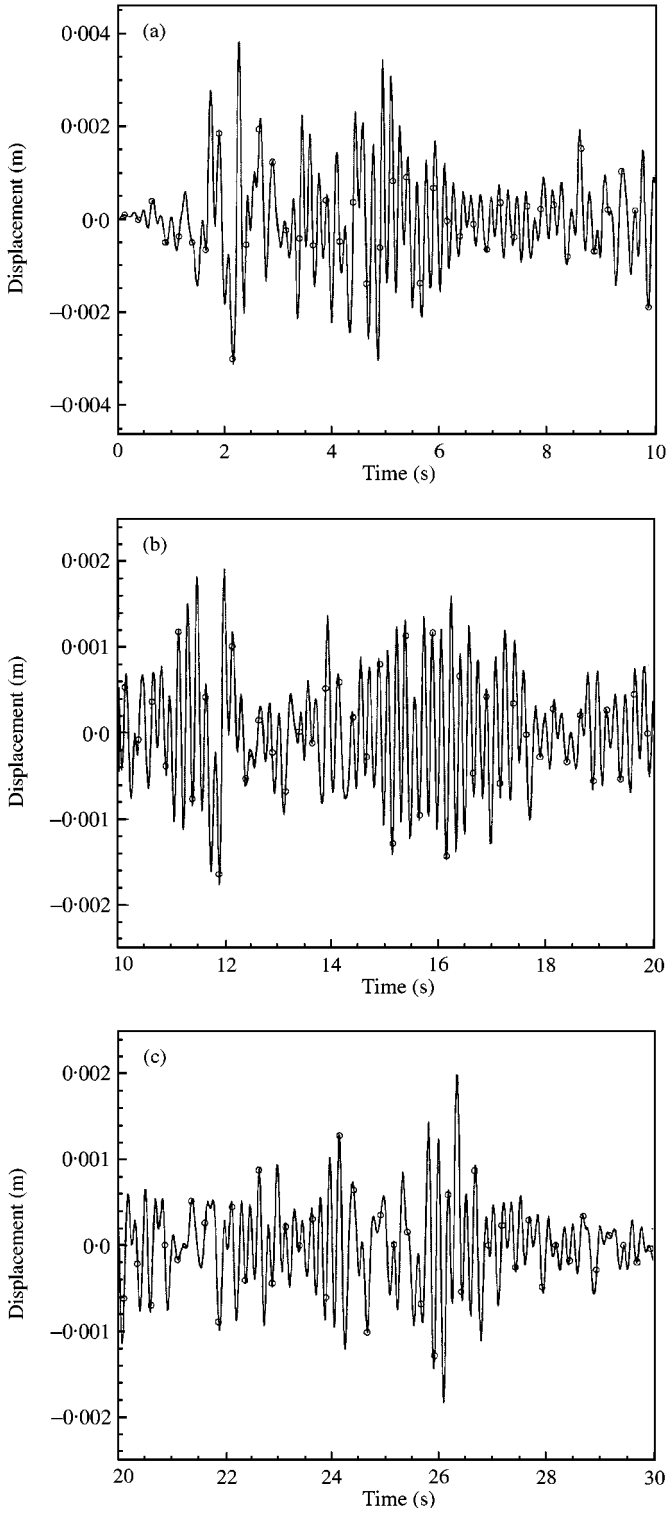

Figure 18. Vertical displacement at the center of the bridge with Rayleigh damping: —○—, Newmark; -----, DAM. (a) 0 < time < 10; (b) 10 < time < 20; (c) 20 < time < 30; (d) 30 < time < 40; (e) 40 < time < 55.

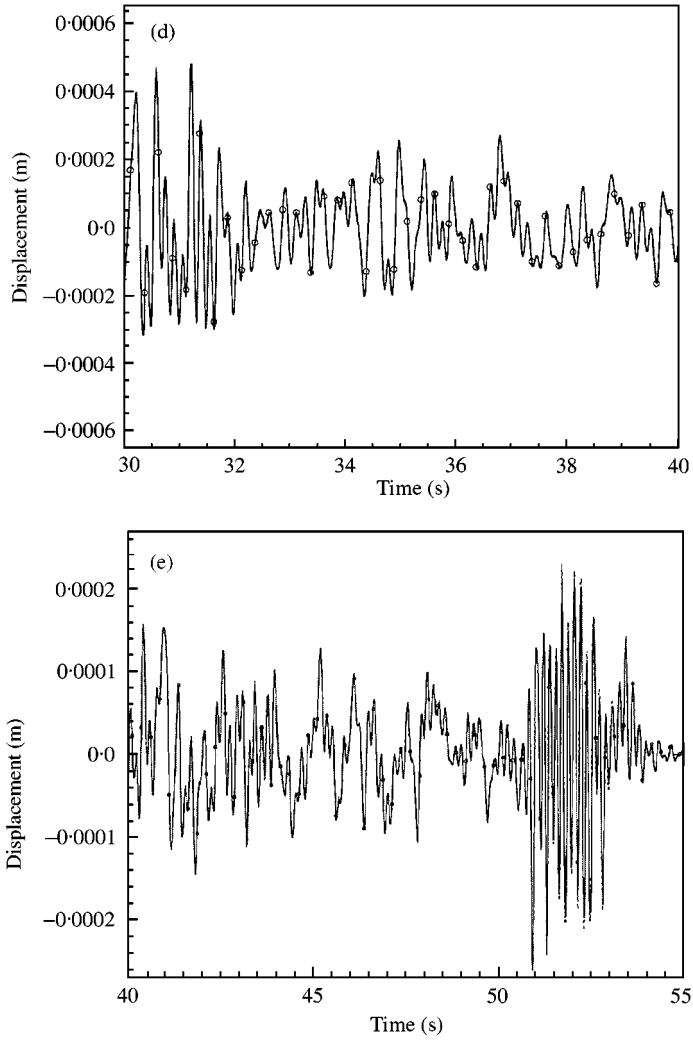

Figure 18. Continued.

In the next example, we calculate displacements of the bridge by neglecting damping. Figures 19(a–k) give the vertical displacement at the center of bridge versus time.

We note that during the first 5 s, the solution obtained with the Newmark-β method and the asymptotic method are practically the same. Where there are strong non-linearities in the loading, namely in the interval (5, 25) s, the solutions do not agree. To obtain a better solution with the Newmark-β method and in order to get the same solution as the one obtained with the asymptotic method, we have taken a time step equal to $T_3/170$.

We will now examine computing time (excluding the time needs to estimate eigenvalues and eigenvectors) and the number of steps required by both methods. In order to choose the most adapted value for the tolerance needed to evaluate critical time for the asymptotic method for different orders of displacement series, we have taken several values and we

Figure 19. Vertical displacement at the center of the bridge (undamped case): —○—, Newmark; -----, DAM. (a) $0 < \text{time} < 5$; (b) $5 < \text{time} < 10$; (c) $10 < \text{time} < 15$; (d) $15 < \text{time} < 20$; (e) $20 < \text{time} < 25$; (f) $25 < \text{time} < 30$; (g) $30 < \text{time} < 35$; (h) $35 < \text{time} < 40$; (i) $40 < \text{time} < 45$; (j) $45 < \text{time} < 50$; (k) $50 < \text{time} < 55$.

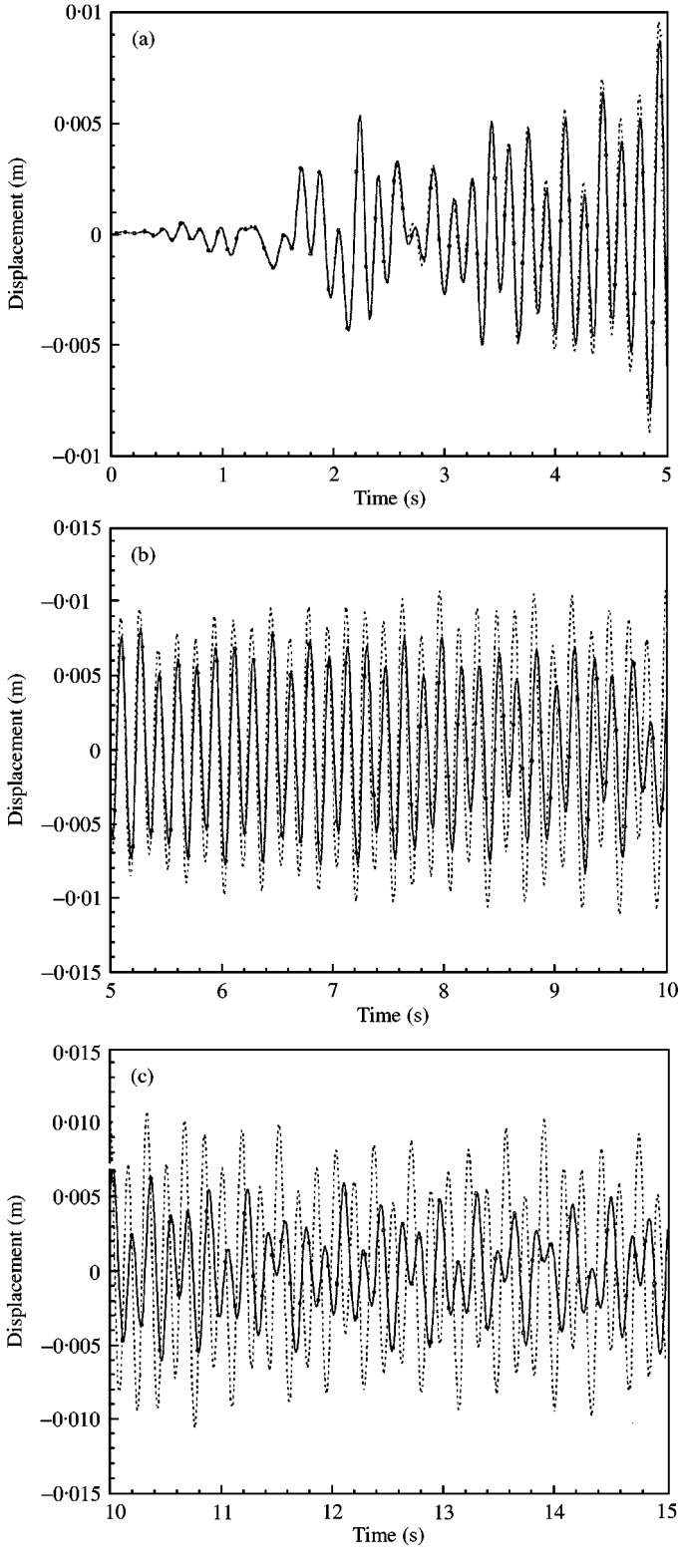
(a)
Displacement (m)
0·01
0·005
0
−0·005
−0·01
0
1
2
3
4
5
Time (s)
(b)
Displacement (m)
0·015
−0·01
0·005
0
−0·005
−0·01
−0·015
5
6
7
8
9
10
Time (s)
(c)
Displacement (m)
0·015
0·010
0·005
0
−0·005
−0·010
−0·015
10
11
12
13
14
15
Time (s)

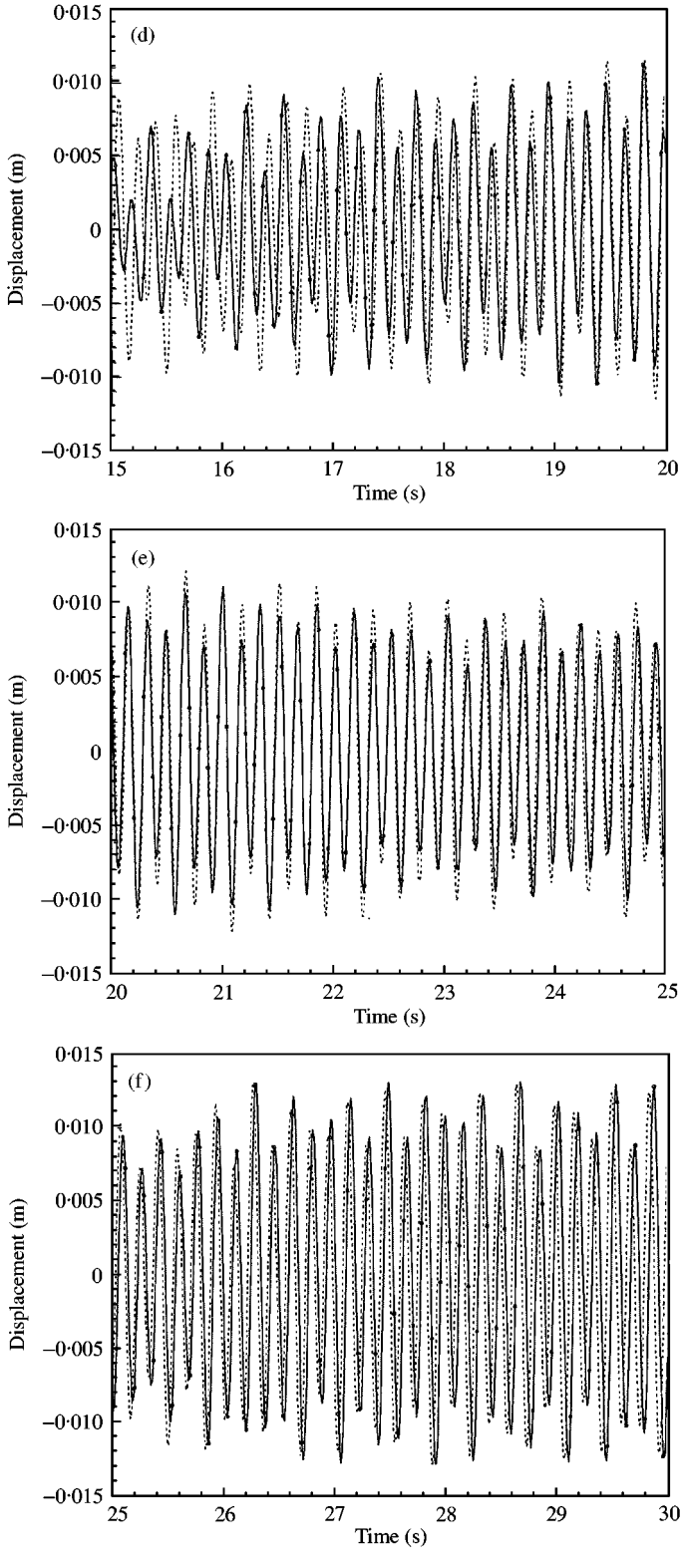

Figure 19. Continued.

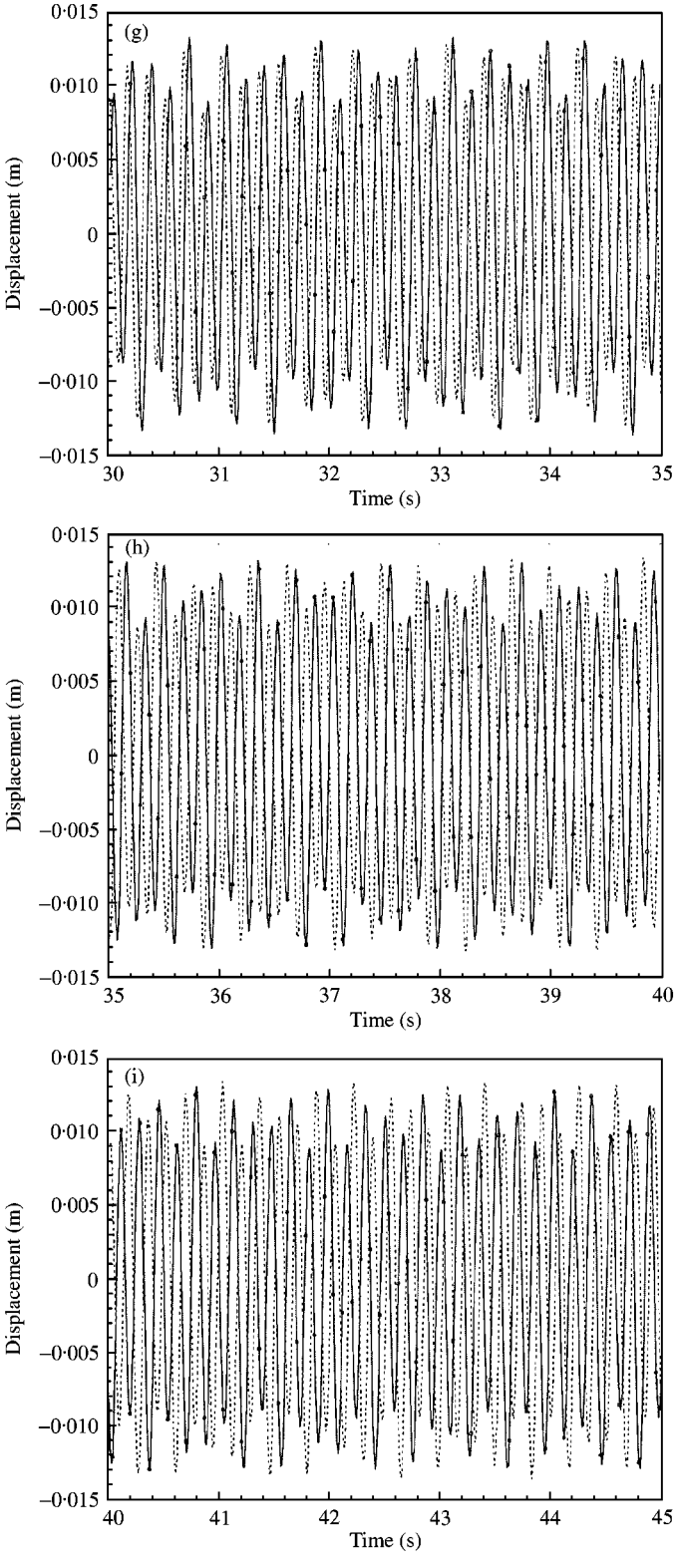

Figure 19. Continued.

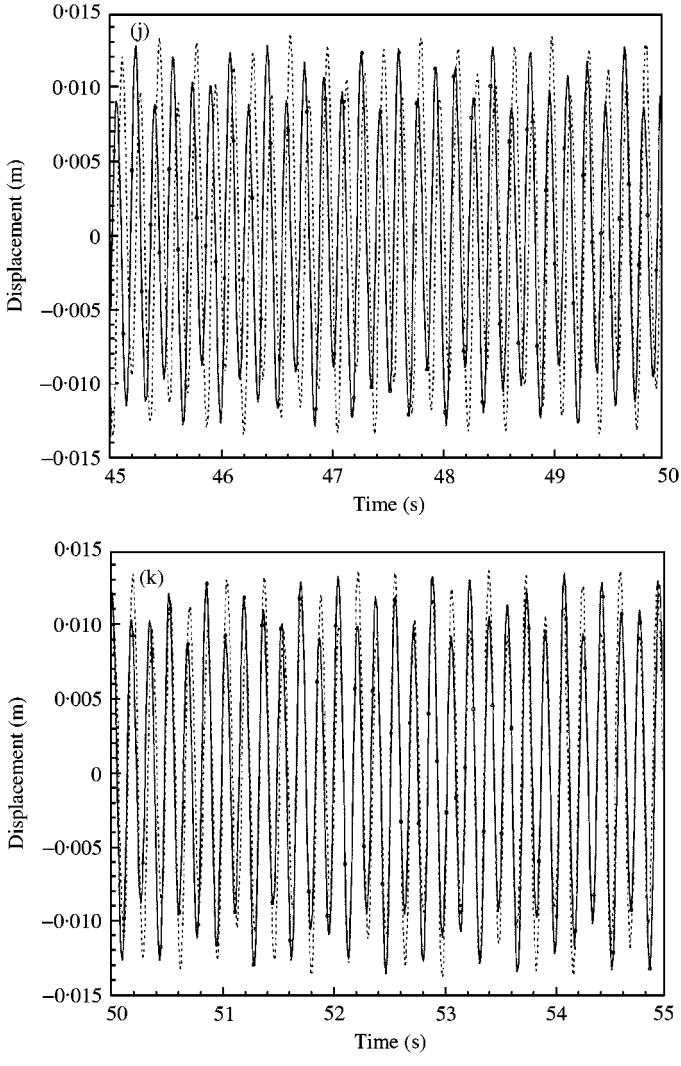

Figure 19. Continued.

selected the most suitable one which gives the critical time which remains inside the radius of convergence. The results are presented in Tables 3–6.

We note from Tables 3 and 5 that the asymptotic method needed fewer time steps than the Newmark-β method to obtain the solution. For the damped case, the Newmark-β method is faster than the asymptotic method. However, for the undamped case and for the same precision level, the asymptotic method with $N = 15$ and 10 is faster than the method of Newmark-β.

We note from Tables 4 and 6 that the asymptotic method is more time consuming for order higher than 15. Table 4 indicates that the asymptotic method is more time consuming for $N = 10$ than 15, because with $N = 10$, we have less coefficients to be computed for the loading but critical time will decrease; however, for $N = 15$, we compute more coefficients for the loading but the critical time is larger and it means that we need less steps to obtain all the solutions. Thus, an optimum order N would have to be found for computing less

TABLE 3

Various time steps of the two computing methods: damped case

Method		Time segment (s)			Total number of step
DAM	$N = 29$, $\varepsilon = 10^{-8}$	Mean 0·016511	Max 0·070266	Min 0·000001	3286
	$N = 20$, $\varepsilon = 10^{-6}$	0·02603	0·064336	0·000047	2077
	$N = 15$, $\varepsilon = 10^{-5}$	0·03555	0·061937	0·000132	1546
	$N = 10$, $\varepsilon = 10^{-5}$	0·02286	0·057136	0·000596	2406
Newmark ($\beta = 1/6$)			0·01		5500

TABLE 4

CPU time: damped case

Method		Time (CPU)	Relative time
DAM	$N = 29$	1 h 14′	24·7
	$N = 20$	23′	7·67
	$N = 15$	10′	3·33
	$N = 10$	11′	3·67
Newmark ($\beta = 1/6$)		3′	1

TABLE 5

Various time steps of the two computing methods: undamped case

Method		Time segment (s)			Total number of step
DAM	$N = 29$, $\varepsilon = 10^{-18}$	Mean 0·005501	Max 0·041827	Min 0·000004	9964
	$N = 20$, $\varepsilon = 10^{-12}$	0·01691	0·04056	0·000014	3252
	$N = 15$, $\varepsilon = 10^{-9}$	0·02154	0·05612	0·000006	2552
	$N = 10$, $\varepsilon = 10^{-8}$	0·01544	0·04047	0·000118	3560
Newmark ($\beta = 1/6$)			0·001		55 000

TABLE 6

CPU time: undamped case

Method		Time (CPU)	Relative time
DAM	$N = 29$	3 h 59′	7·46
	$N = 20$	33′	1·03
	$N = 15$	18′	0·56
	$N = 10$	13′	0·41
Newmark ($\beta = 1/6$)		32′	1

coefficients of the loading and less steps in order to minimize the computing time. The tolerance taken is very small for the undamped case due to the strong amplitude of the displacement curve. According to this parametric study, we can see that the optimum order for this problem is $N = 15$. We note that in Zahrouni's work [9], the suggested optimum order is also 15.

5. CONCLUSION

In this paper, we have studied linear dynamic problems for arbitrary loading solved using the asymptotic method. For the representation of an arbitrary loading, we have started with the Fourier series. This approach is often applied for the periodic functions. Unfortunately, in practice, we seldom have this kind of loading. We thus prefer to take advantage of the Fourier integral which is an extension of the Fourier series to unperiodic functions. We have shown that, using these two techniques, the asymptotic method converges towards the exact solution. However, we have observed that, exploiting the Fourier integral, we have saved computing time and increased also the critical time compared to the Fourier series. Then, we have extended the asymptotic method associated with the Fourier integral to study more complex problems such as seismic analysis.

The results of the numerical analyses carried out for several examples have proved that the asymptotic method gives a good approximation of the exact solution and it has a better estimation of the response compared to the Newmark-β method. This is due to its ability to capture the loading non-linearities. Another advantage of this method is that it requires fewer time segments than the classical time integration schemes. The time segment length of the asymptotic method is automatically computed and adapted according to the loading variation. It decreases when these exist strong variations of the loading and it increases when the loading becomes regular. According to examples presented in this paper, we suggest an optimum order of 15 for the displacement series. As any numerical method, the asymptotic method presents some disadvantages. This method is conditionally stable and the representation of complex loading by using the Fourier integral is relatively time consuming. Thus, we propose to approach the time segments of the loading linearly in such a way that between two points, we will have $f(t) = at + b$. In this case, the time step could be conditioned by the length of the time segment. This possibility would be interesting to compare to the use of the Fourier integral when we consider computing time. Another possibility is to carry out polynomial approximations for several segments of time. For example, we can construct a quadratic approximation for two consecutive segments.

The asymptotic method has already proved its effectiveness for static non-linear problems. However, this method remains unexploded in non-linear dynamics. We believe that it would be interesting to explore the asymptotic method in this domain.

ACKNOWLEDGMENT

Support of the Natural Sciences and Engineering Research Council (NSERC) from the Canadian government and Fonds FCAR from the Quebec government are gratefully acknowledged for the partial financial support of this research project. The Democratic Algerian Republic financially supported the first author of this paper.

REFERENCES

1. C. LANCZOS 1956 *Applied Analysis*. Englewood Cliffs, NJ: Prentice-Hall.
2. B. COCHELIN 1994 *Ph.D. Thesis, University of Metz, France*. Numerical asymptotic method for the geometrically non-linear analysis of elastic structures (in French).
3. B. BUDIANSKY 1974 *Advances in Applied Mechanics* **14**, 1–65. Theory of buckling and post-buckling behavior of elastic structures.
4. M. POTIER-FERRY 1987 *Lecture Notes in Physics* **288**, 1–82. Foundations of elastic post-buckling theory, in buckling and bost-buckling.
5. J. M. T. THOMPSON and A. C. WALKER 1968 *International Journal of Solids and Structures* **14**, 757–768. The non-linear perturbation analysis of discrete structural systems.
6. R. H. GALLAGHER 1975 *Computational Mechanics—Lecture Notes in Mathematics* **406**, 75–79. Perturbation procedures in non-linear finite element structural analysis.
7. N. DAMIL and M. POTIER-FERRY 1990 *International Journal of Engineering Sciences* **28**, 943–957. A new method to compute perturbed bifurcation: application to buckling of imperfect elastic structures.
8. S. AMMAR 1996 *Ph.D. Thesis, Department of Civil Engineering, Laval University, Quebec, Canada*. Perturbed asymptotic method applied to non-linear problem with large rotations (in French).
9. H. ZAHROUNI 1998 *Ph.D. Thesis, University of Metz, France*. Numerical asymptotic method for the shells in large rotations (in French).
10. M. FAFARD, K. HENCHI, G. GENDRON and S. AMMAR 1997 *Journal of Sounds and Vibrations* **208**, 73–99. Application of an asymptotic method to transient dynamic problems.
11. R. W. CLOUGH and J. PENZIEN 1993 *Dynamics of Structures*. New York: McGraw-Hill.
12. K. J. BATHE and E. W. WILSON 1976 *Numerical Methods in Finite Element Analysis*. Englewood Cliffs, NJ: Prentice-Hall.
13. E. DIONNE 1997 *Master Thesis, Department of Civil Engineering, Laval University, Quebec, Canada*. Asymptotic method applied to the temporal resolution of the linear dynamic equations. (in French).
14. H. T. A. LAU 1995 *Numerical Library in C for Scientists and Engineers*. Boca Raton, FL: CRC Press.
15. N. BERRAHMA-CHEKROUN 1998 *Master Thesis, Department of Civil Engineering, Laval University, Quebec, Canada*. Study of various loading types for linear dynamic problems solved by the asymptotic method. (in French).

APPENDIX A: NOMENCLATURE

$[C]$	damping matrix
$\{F\}$	load vector
$\{F_i\}$	vector containing coefficients i of the loading polynomial
$[K]$	rigidity matrix
ℓ	upper limit of the Fourier integral
L	length
$[M]$	mass matrix
N	polynomial order
$R(t)$	residue
$\{R_i\}$	vector containing coefficients i of the residue polynomial
t_{cr}^i	critical time i
u	displacement
$\dot{u}$	velocity
$\ddot{u}$	acceleration
$\{u_i\}$	vector containing coefficients i of the displacement polynomial
Δt	time step
ε	tolerance
t; τ	time
Ω_n	frequency of the Fourier series
a_0, a_n, b_n	Fourier coefficients